Corrosion Inhibition of Mild Steel in 1 M HCl Solution by *Xylopia Ferruginea* Leaves from Different Extract and Partitions

W.A.W. Elyn Amira[1], *A.A. Rahim*[1,*], *H. Osman*[1], *K. Awang*[2], *P. Bothi Raja*[1]

[1] School of Chemical Sciences, University Sains Malaysia, 11800 Penang, Malaysia.
[2] Department of Chemistry, Faculty of Science, Universiti Malaya, 50603 Kuala Lumpur, Malaysia.
[*]E-mail: afidah@usm.my

The influence of *Xylopia ferruginea* leaves extract and partitions in different solvents on the corrosion behavior of mild steel (MS) in 1 M HCl was studied using weight loss, potentiodynamic polarization, electrochemical impedance spectroscopy (EIS) and Scanning Electron Microscope (SEM) techniques. The results revealed that *Xylopia ferruginea* was an excellent green inhibitor and the inhibition efficiencies obtained from weight loss and electrochemical experiments were in good agreement. Potentiodynamic polarization studies clearly reveal that all inhibitors behaved as mixed-type inhibitors with predominant anodic effectiveness. The Nyquist plots showed that on increasing the inhibitor concentration, the charge transfer resistance increased and the double layer capacitance decreased. The adsorption of inhibitors on MS surface obeys the Langmuir adsorption isotherm. SEM studies confirmed that the corrosion protection of MS was by the adsorption of inhibitors. The effectiveness as corrosion inhibitors is in the order of chloroform partition (CP) > *n*-hexane partition (HP) > methanol extracts (ME).

1. INTRODUCTION

Corrosion is a very common phenomenon in industries and it has wide amount of interest because of its hazardous nature on metals [1]. Due to the excellent mechanical properties and low cost, mild steel is extensively used as a constructional material in many industries. However, when exposed to the corrosive industrial environment, it is easily corroded. Normally, acid solutions such as hydrochloric acid are widely used such as in acid pickling, industrial cleaning, oil well cleaning, etc. The use of inhibitors is one of the most practical methods for protection against corrosion to protect

metal dissolution and acid consumption [2]. Synthetic organic compounds [3-5] and organic compounds which can be extracted from natural resources could serve as effective corrosion inhibitors due to the presence of polar functions with S, O, or N atoms in the molecule, heterocyclic compounds and π electrons [6-11]. Recently the use of synthetic inhibitors has created environmental problems due to its toxicity properties. Therefore researchers are now focusing on development of cheap, non-toxic and environmental friendly corrosion inhibitors from natural products. These natural organic inhibitors that can be extracted or synthesized from potential herbs, spice and medicinal plants can be used as corrosion inhibitors of mild steel in acidic solution due to its active chemical activity, low toxicity and low cost [12-15].

Alkaloids are naturally occurring chemical compounds containing basic nitrogen atoms which are produced by a large variety of organisms, including bacteria, fungi, plants, and animals. Many plants are known to produce various types of alkaloids [16, 17]. Alkaloids such as papaverine, strychnine, quinine, piperine, liriodenine, oxoanalobine and nicotine were also studied as corrosion inhibitors in acid medium [18-20]. The genus *Xylopia* is distributed in tropical Africa and Malaysia [21]. *X. ferruginea* is a species of plants in the *Annonaceae* family. It is a medium sized forest tree which can reach up 10 to 20 meters in height. *X. ferruginea* is easily found in Peninsular Malaysia except in Perlis, Penang and Seberang Prai. It is also distributed in Thailand, Borneo and Sumatera [22]. The extracts of this plant, which contains numerous naturally environmental organic compounds, may be utilized as natural corrosion inhibitors. The genus *Xylopia* is known to contain alkaloids of aporphine and tetrahydroberberine types and specifically *X. ferruginea* extracts contain significant amount of atheroline alkaloids [23]. In this paper, the corrosion inhibitor property of alkaloids in different solvent extract and partition of *X. ferruginea* leaves on mild steel in 1 M HCl was investigated by weight loss, potentiodynamic polarization, EIS and SEM techniques.

2. EXPERIMENTAL

2.1. Materials

Mild Steel (MS) of the following composition (wt. %: 0.039 % P; 0.06% Si; 0.55% Mn; 0.205% C; Fe balance) were used in this studies. The MS specimens were mechanically cut into dimensions of 30.0 x 10.0 x 1.00 mm for weight loss studies and 30.0 x 30.0 x 1.00 mm for electrochemical studies. Prior to all measurements, the specimens were polished successively with a series of emery paper (grade 350, 500, 800, 1000, 1200 and 1500). Then, the specimens were washed with double distilled water and acetone (AR grade) and dried at room temperature (27±2 °C). The 1 M HCl solution was prepared by dilution of analytical grade 37% HCl with double distilled water.

2.2. Inhibitors preparation

Air-dried leaves of *X. ferruginea* (1.0 kg) were pulverized into fine powder and extracted exhaustively with methanol at room temperature (27±2 °C). Concentration of the combined methanol

extracts yielded a dark green crude extract of methanol extract (ME) (214.5 g). This extract was suspended in methanol:water (l:2) overnight and successively partitioned with *n*-hexane (yield 6.3 g) to yield the *n*-hexane partition (HP). The remaining aqueous extract was partitioning again with chloroform to yield the chloroform partition (CP) (4.1 g). These ME, HP, and CP was used for the corrosion inhibitor studies. The maximum solubility of extracts in 1 M HCl was found to be 500 ppm. All inhibitors were dissolved in 1 M HCl at different concentrations ranging from 50 ppm to 500 ppm. The 1 M HCl solution in the absence of inhibitors was taken as blank for comparison.

2.3. Weight loss measurements

MS specimens were immersed in triplicate in 100 mL of the test solutions (1 M HCl) with and without addition of inhibitors of different concentrations at room temperature (27±2 °C). The cleaned specimens were weighed before and after 2 hours of immersion in the test solution. The percentage inhibition efficiency (%IE) was calculated by Eq. (1).

$$\%IE = \frac{W_{(o)} - W_{(i)}}{W_{(o)}} \times 100 \qquad (1)$$

Where, $W_{(o)}$ is the weight loss of MS without inhibitor and $W_{(i)}$ is the weight loss of MS with inhibitor.

2.4. Electrochemical measurements

Electrochemical studies were carried out using Gamry Instruments reference 600 (potentiostat/galvanostat/ZRA). A classical three electrode system was used for these studies. Mild steel specimens were used as a working electrode, platinum (Pt) electrode and saturated calomel electrode (SCE) served as auxillary and reference electrodes, respectively. All electrochemical experiments were conducted at room temperature (27±2 °C) using 100 mL of test solution. Before the potentiodynamic polarization (Tafel) and electrochemical impedance spectroscopy (EIS) experiments, the electrode was allowed to corrode freely and its open circuit potential (OCP) was recorded as a function of time up to 30 min.

AC impedance measurements were carried out at the corrosion potential (E_{corr}) with frequency range from 100,000 to 0.1 Hz at an amplitude of 10 mV and scan rate of 10 points per decade. The impedance diagrams are given in Nyquist representation. The electrical equivalent circuit for the system was obtained. The %IE was calculated from the charge transfer resistance (R_{ct}) values by using the Eq. (2).

$$\%IE = \frac{R_{ct(i)} - R_{ct(o)}}{R_{ct(i)}} \times 100 \qquad (2)$$

Where, $R_{ct(o)}$ is the charge transfer resistance of MS without inhibitor and $R_{ct(i)}$ is the charge transfer resistance of MS with inhibitor.

The Tafel polarization curves were recorded by scanning the electrode potential from -300 mV to 300 mV (*vs* SCE) with a scanning rate of 1 mV/s. The linear Tafel segments of the anodic and cathodic curves were extrapolated to corrosion potential to obtain the corrosion current densities (I_{corr}). The %IE was obtained from Eq. (3).

$$\%IE = \frac{I_{corr(o)} - I_{corr(i)}}{I_{corr(o)}} \times 100 \qquad (3)$$

Where, $I_{corr(o)}$ is the corrosion current densities of MS without inhibitor and $I_{corr(o)}$ is the corrosion current densities of MS with inhibitor.

2.5 Fourier transform infrared spectroscopy (FTIR) analyses

All inhibitors were characterized by FTIR spectroscopy for identification of the active functional groups. The FTIR study was carried out by using the Perkin Elmer System 2000 FTIR instrument.

2.6 Scanning Electron Microscope (SEM) analyses

SEM LEO SUPRA 50VP - Scanning Electron Microscope was used for monitoring the surface morphological changes. For this study, finely polished MS plates were immersed in 1 M HCl solution in the presence and absence of 500 ppm of green inhibitors for 2 h. Then the specimens were cleaned with distilled water and acetone, dried in cold air blaster and used for the analysis.

3. RESULTS AND DISCUSSION

3.1 Weight loss measurements

The inhibition efficiency of MS exposed to 1 M HCl at room temperature (27±2 °C) as a function of concentration of different inhibitors is shown in Figure 1 and Table 1. It is observed that the inhibition efficiency of MS increased with increasing concentrations of inhibitors. This behavior could be attributed to the increase in adsorption of inhibitor on the metal or at the solution interface on increasing its concentration. The highest %IE was 82, 88 and 94% for ME, HP and CP respectively. Comparison of the inhibition efficiencies of inhibitors shows that the efficiencies followed the trend: CP > HP > ME. This is due to the high alkaloids chemical constituents in CP that can be adsorbed onto the MS surface. The higher yield of creamy precipitate for Mayer's test was obtained for CP compared to NP and ME, which indicated that CP contained the highest alkaloids content.

Table 1. Inhibition efficiency (%IE) values for the corrosion of MS in 1 M HCl in the absence and presence of different concentrations of inhibitors from weight loss measurement at 27±2 °C for 2 h of immersion time.

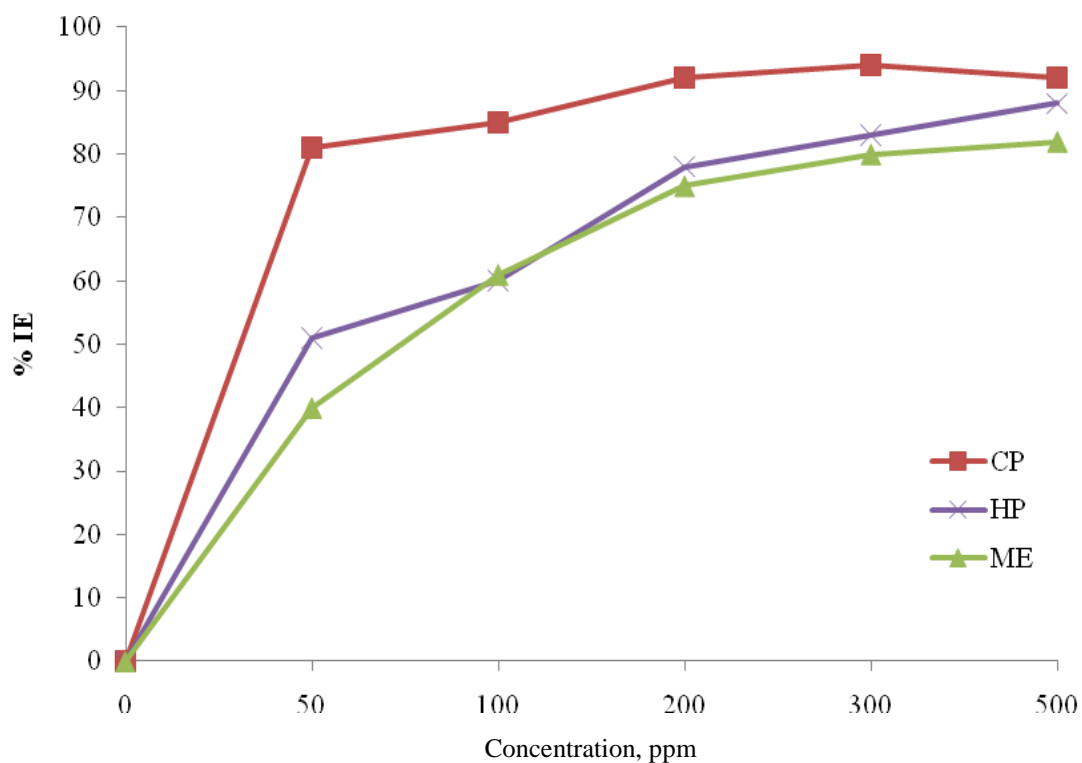| Inhibitors	Concentrations (ppm)	Weight loss (g)	%IE
ME	0	0.0174	-
	50	0.0104	40
	100	0.0069	60
	200	0.0043	75
	300	0.0035	80
	500	0.0031	82
HP	0	0.0180	-
	50	0.0089	51
	100	0.0072	60
	200	0.0040	78
	300	0.0030	83
	500	0.0021	88
CP	0	0.0203	-
	50	0.0039	81
	100	0.0030	85
	200	0.0015	92
	300	0.0013	94
	500	0.0016	92

Figure 1. Percentage inhibition (%IE) of different inhibitors in 1 M HCl from the weight loss method

3.2 Polarization measurements

The potentiodynamic polarization curves obtained from the corrosion behavior of MS in 1 M HCl in the absence and presence of green inhibitors are shown in Figures 2, 3, and 4. The electrochemical parameters; corrosion potential (E_{corr}), corrosion current density (I_{corr}), anodic and cathodic Tafel slopes (β_a and β_c) were calculated from the intersection of the anodic and cathodic Tafel lines of the polarization curves at E_{corr}. All the parameters obtained from the polarization measurements are listed in Table 2. %IE was calculated by using Eq. (3).

From the potentiodynamic polarization curves, it can be clearly seen that when compared with the blank, both anodic and cathodic curves were shifted toward the direction of lower current density for all inhibitors as the concentration increased. This phenomenon implied that the inhibitors could suppress the anodic reaction of metal dissolution of iron and cathodic hydrogen evolutions [24]. Moreover, increase in concentration of inhibitors did not change significantly the β_a and β_c slopes, signifying that the inhibition mechanism also occurred by simple blocking of the available anodic and cathodic sites of the MS surface.

Table 2. Electrochemical polarization parameters for the corrosion inhibitor study of MS in 1 M HCl in the absence and presence of different concentrations of inhibitors.

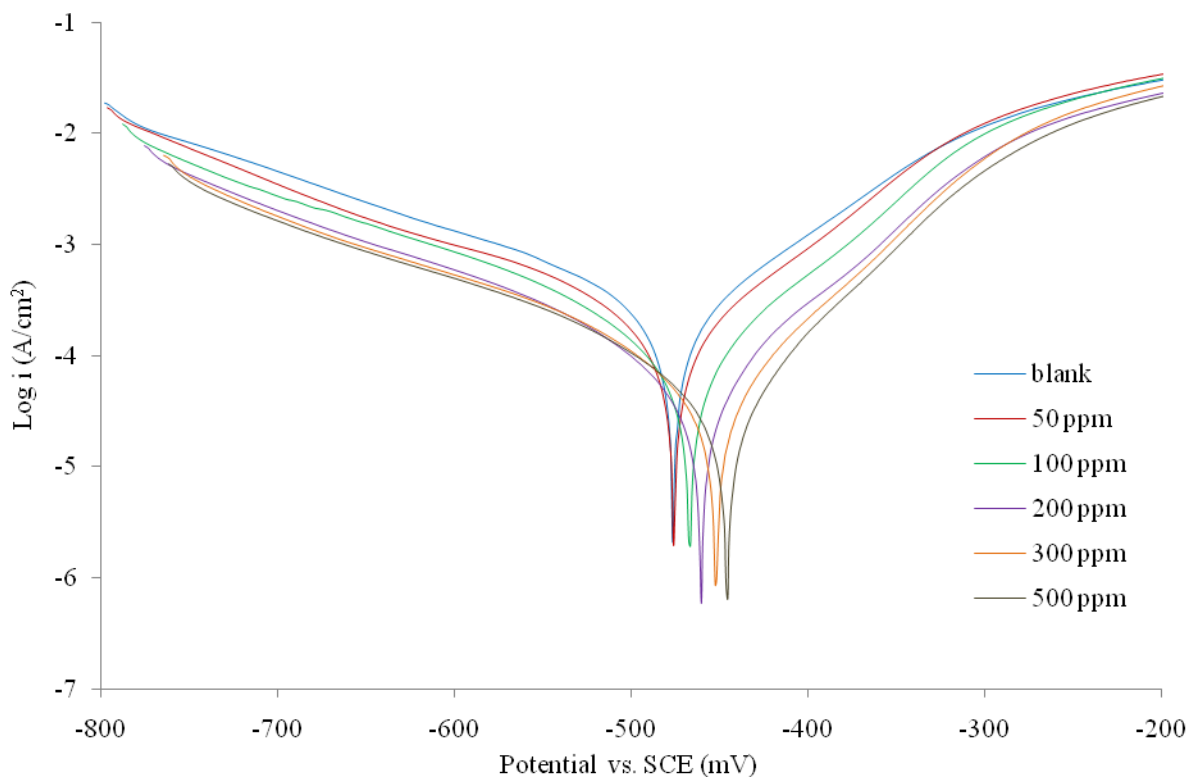| Inhibitors	Concentrations (ppm)	β_a(mV/dec)	$-\beta_c$(mV/dec)	E_{corr} (mV)	I_{corr} (μA/cm^2)	%IE
ME	0	96	110	-478	178	-
	50	80	100	-475	112	37
	100	70	87	-468	63	65
	200	65	65	-460	38	77
	300	60	83	-452	32	82
	500	55	85	-445	25	86
HP	0	96	110	-478	178	-
	50	77	106	-472	96	46
	100	77	103	-472	89	50
	200	67	103	-462	62	65
	300	67	105	-450	45	75
	500	53	97	-428	22	87
CP	0	96	110	-478	178	-
	50	66	90	-468	38	79
	100	65	92	-460	26	85
	200	67	68	-452	21	88
	300	63	97	-438	20	89
	500	55	105	-425	16	91

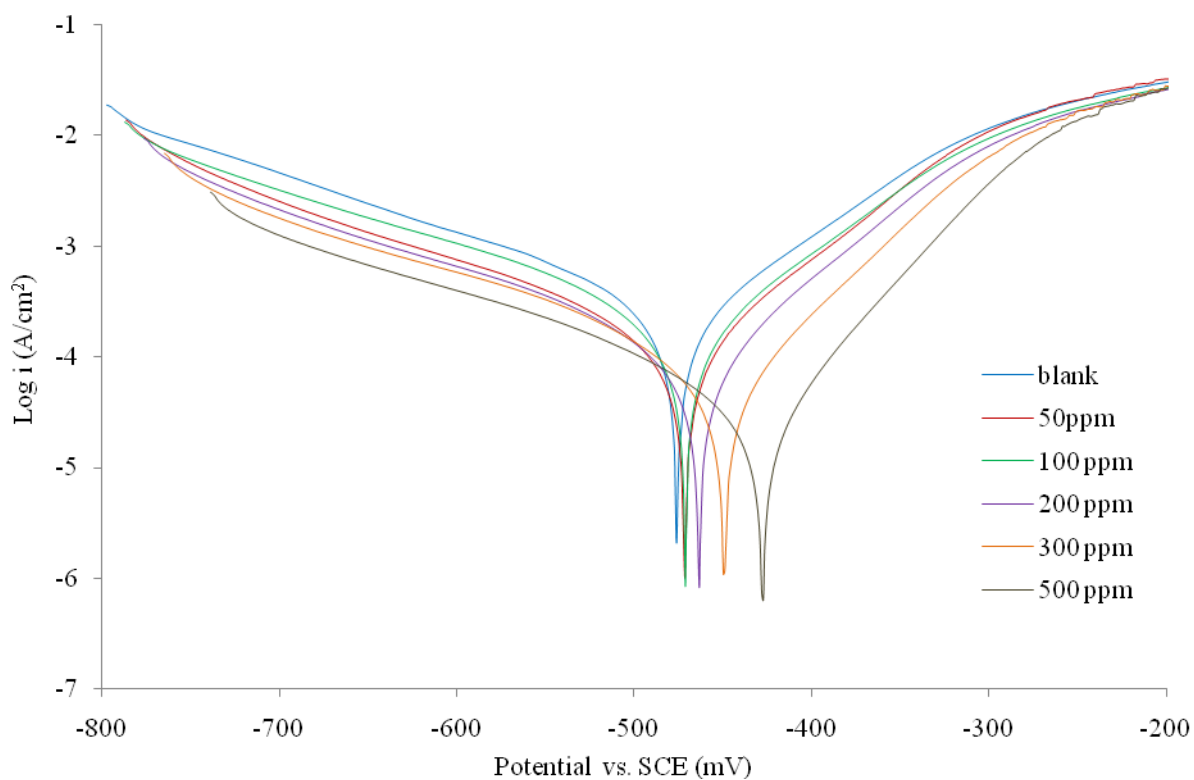**Figure 2.** Tafel plot of MS immersed in 1 M HCl with and without ME

Figure 3. Tafel plot of MS immersed in 1 M HCl with and without HP
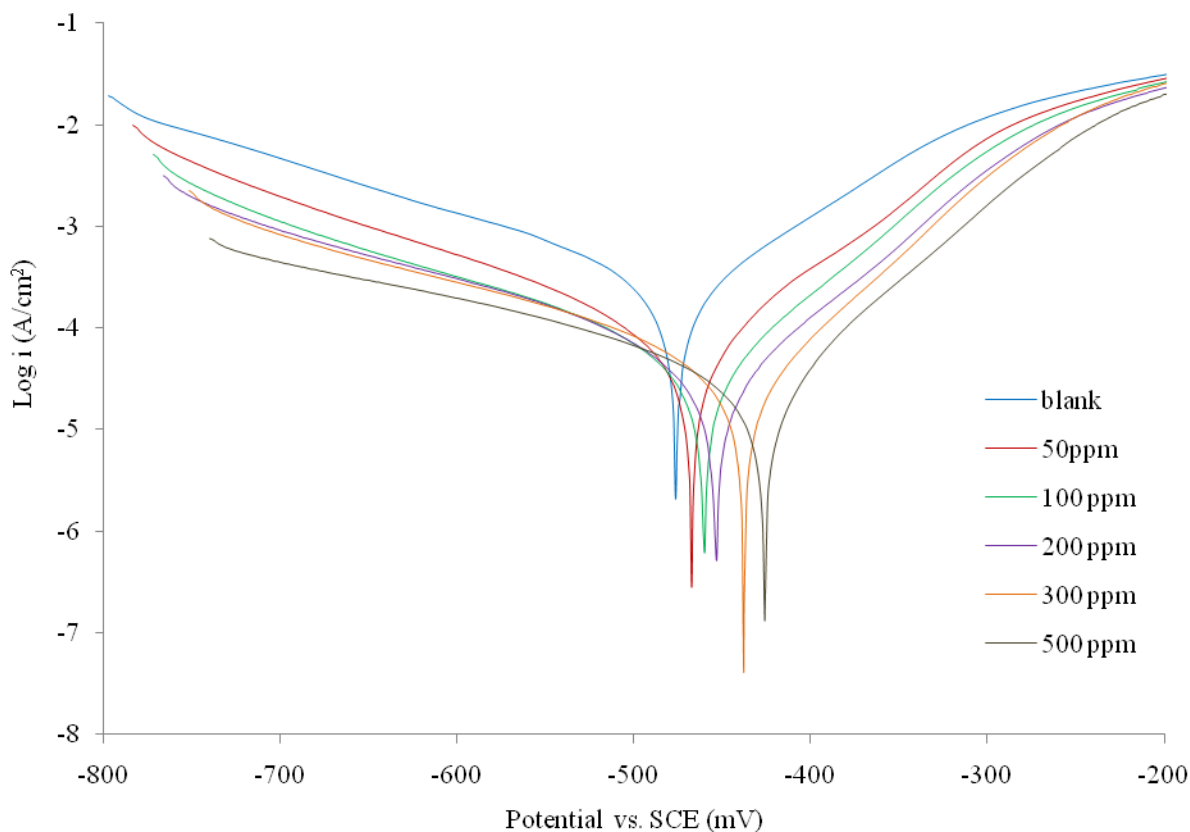
Figure 4. Tafel plot of MS immersed in 1 M HCl with and without CP

In the presence of inhibitors, the E_{corr} of mild steel shifted 3-53 mV anodically compared to the blank. This indicates that the inhibitor reduce the corrosion rates predominantly by dissolution of metal (anodic mode). The inhibitors may shift the equilibrium of corrosion process to the passive direction causing a formation of thin passivation oxide film over the anodic sites, which may increase the anodic potential and depressed the oxidation process. From previous study, it was reported that an inhibitor can be classified as cathodic or anodic type if the displacement in the E_{corr} is more than 85mV with respect to E_{corr} of the blank [25]. Thus, this reveals that all inhibitors act as mixed-type inhibitor with predominant anodic effectiveness.

From Table 2, the inhibition of these reactions was more pronounced on the increasing of inhibitor concentration for all inhibitors, reaching values of 86, 87 and 91% for ME, HP and CP, respectively. The maximum inhibition of 91% was obtained for 500 ppm CP in 1 M HCl solution.

3.3. Electrochemical impedance spectroscopy (EIS) measurements

The Nyquist plots for MS in 1 M HCl in the absence and presence of green inhibitors are shown in Figures 5, 6 and 7. Nyquist impedance plots were analysed by fitting the experimental data to a simple circuit model, Figure 8, that includes the solution resistance (R_s), charge transfer element (R_{ct}) constant phase element (CPE) and surface inhomogeneity (*n*) and the values are depicted in Table 3.

Figure 5 shows depressed Nyquist plots which are not perfect semicircles as expected from the theory of EIS. This difference can be explained by non-ideal behaviour of double layer as a capacitor. Therefore it is necessary to use a constant phase element, CPE, instead of double layer capacity to account for non-ideal behaviour. This CPE, which is considered as a surface irregularity, causes a greater depression in Nyquist semicircle diagram, where the metal-solution interface acts as a capacitor with irregular surface [26]. The CPE can be modelled as follows [27]:

$$Z_{CPE} = (j\omega C)^{-n}$$ (4)

Where Z_{CPE} is the impedance, j the square root of -1, ω the frequency, C the capacitance and n is a measure of the non-ideality of the capacitor (surface irregularity) and has a value in the range of $0 \le n \le 1$. If the electrode surface is homogeneous and plane, the value of n equals to 1 and the metal-solution interface acts as a capacitor with regular surface.

The Nquist plots in Figures 5, 6 and 7 yield a capacitive loop at high frequencies in the absence and presence of inhibitors, indicating that the corrosion process is mainly controlled by a charge transfer process [28]. It is also observed that the diameters of the capacitive loop increase with increasing green inhibitor concentrations which indicates the increasing coverage of metal surface. Further, it is clear from Table 2 that by increasing the inhibitor concentration, the R_{ct} values increase.

Table 3. Electrochemical impedance parameters for the corrosion of MS in 1 M HCl in the absence and presence of different concentrations of inhibitors.

| Inhibitors	Concentrations (ppm)	R_s ($\Omega.cm^2$)	R_{ct} ($\Omega.cm^2$)	CPE x 10^5 ($\mu F/cm^2$)	n	%IE
ME	0	3.449	109.6	19.62	0.8219	-
	50	2.946	150.6	18.70	0.8206	52
	100	3.094	267.6	17.25	0.8191	59
	200	4.302	451.3	14.85	0.8068	76
	300	3.347	482.7	13.07	0.7996	77
	500	4.087	621.9	12.66	0.7868	82
HP	0	3.449	109.6	19.62	0.8219	-
	50	3.794	138.6	19.14	0.8201	21
	100	3.914	142.2	17.18	0.8087	23
	200	3.761	237.0	14.49	0.8096	54
	300	3.405	362.1	13.56	0.7772	70
	500	2.969	749.3	12.37	0.7346	85
CP	0	3.449	109.6	19.62	0.8219	-
	50	3.429	299.1	14.87	0.8037	63
	100	3.391	622.7	12.99	0.7735	82
	200	3.484	779.5	10.07	0.7349	86
	300	2.983	959.5	9.947	0.7273	89
	500	2.758	1595	9.886	0.5984	93
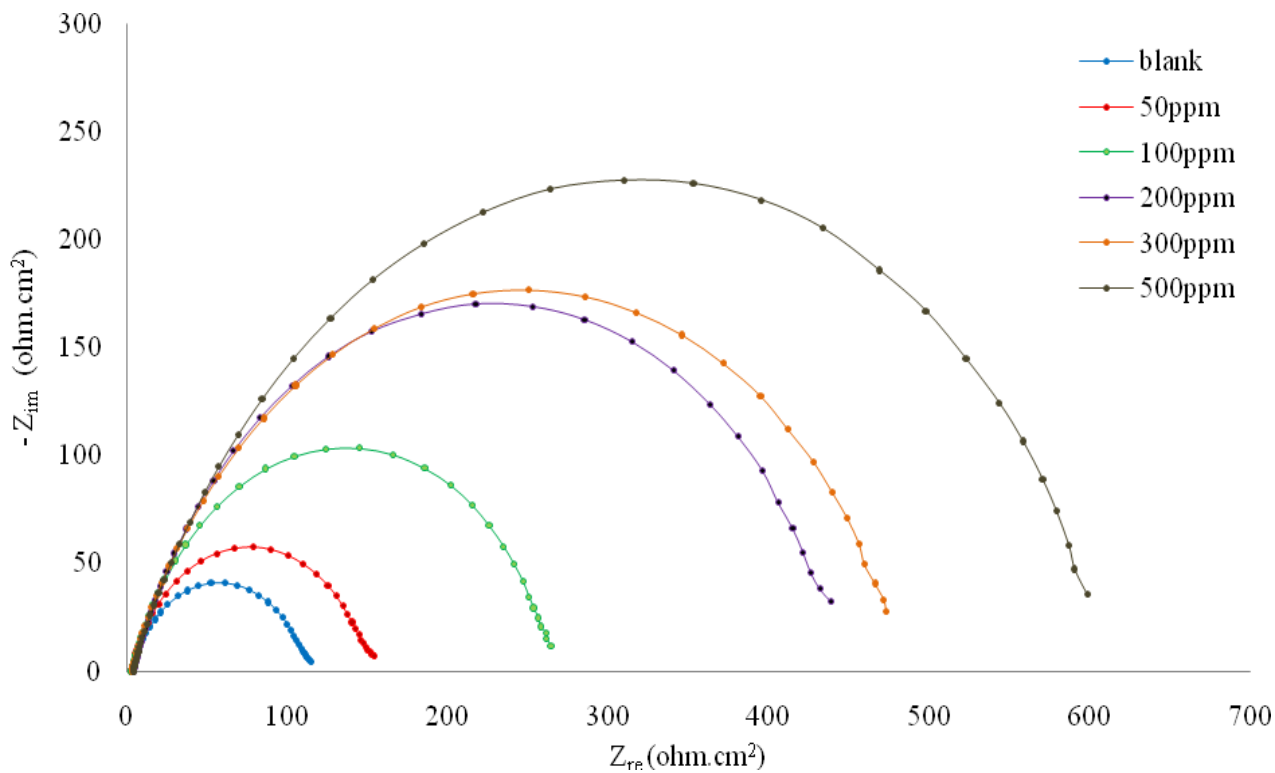
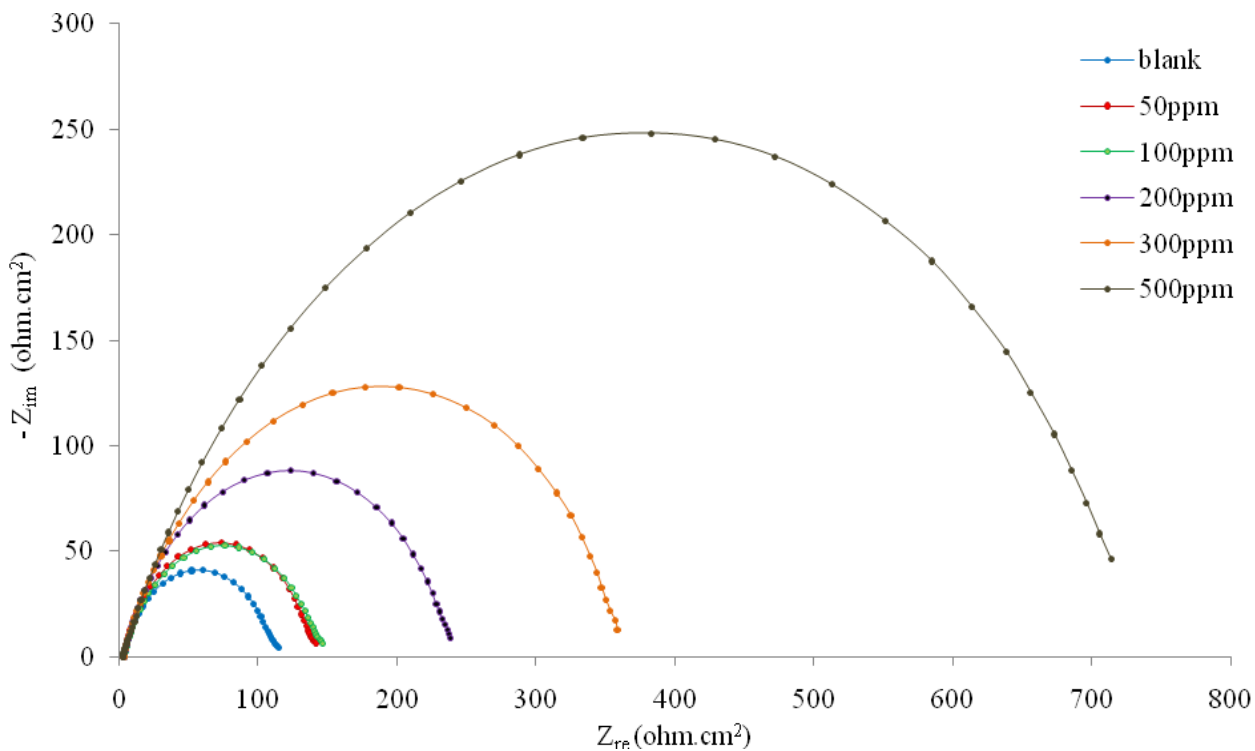**Figure 5.** Nquist plots of MS immersed in 1 M HCl with and without ME

Figure 6. Nquist plots of MS immersed in 1 M HCl with and without HP
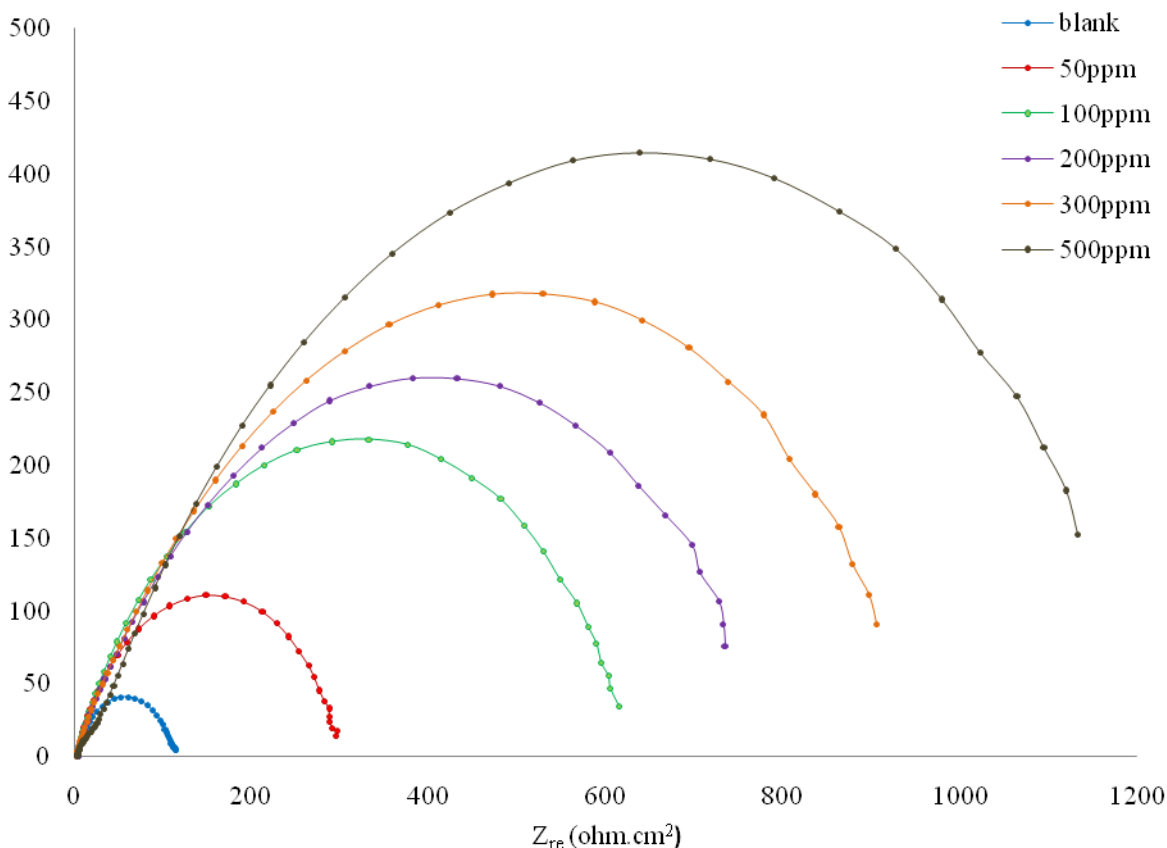
Figure 7. Nquist plots of MS in 1 M HCl with and without CP
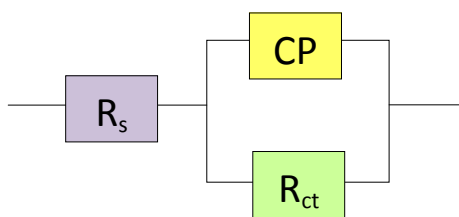

**Figure 8.** Equivalent circuit model for Nyquist plots

This is because, the addition of inhibitor increases the adsorption of phyto-constituents over the metal surface and results in the formation of a protective layer; which may decrease the electron transfer between the metal surface and the corrosive medium. On the other hand, the values of CPE decreased with an increase in inhibitor concentrations and thus the inhibition efficiencies increase. The decrease in CPE values can be attributed to a decrease in local dielectric constant and/or an increase in the thickness of the electrical double layer which leads to an increase in the inhibition efficiency. Therefore it is suggested that the inhibitors act by adsorption at the MS surface or solution interface. Besides, the change in CPE values is caused by the gradual displacement of water molecules by the adsorption of the organic molecules on the MS surface, decreasing the extent of the metal dissolution [29]. The values of *n* (Table 3), ranging between 0.8219 and 0.5984, indicate that the charge transfer

process controls the dissolution mechanism of MS in 1 M HCl solution in the absence and in the presence of the inhibitors [30]. The higher frequency range loops have depressed semi-circular appearance, $0.5 \leq n \leq 1$, which is often referred to as frequency dispersion as a result of the non-homogeneity or the roughness of the metal surface [31, 32]. However, from the Table 3, the decrease in n values as concentration of inhibitors increase is similarly observed by several studies indicated the increase in non-homogeneity of the MS surface [33-35]. However, the increase in non-homogeneity is not related to the roughness or smoothness of the surface of MS as shown by SEM micrographs in Figure 9.

Inhibition efficiency, calculated from the values of R_{ct} (Eq. 2) was found to be maximum at 500 ppm for all inhibitors with %IE 82, 85 and 93% of ME, HP, and CP respectively. In conclusion, the results of the electrochemical studies were in good agreement with the results of gravimetric studies with slight deviations. This is due to the difference in immersion period of MS in the aggressive media [36]. From all studies, the corrosion inhibition ability of all inhibitors is in the order of CP > HP > ME which can be explained due to the alkaloids content.

3.4. SEM analyses

Surface morphology of MS was studied by scanning electron microscopy after 2 h immersion in 1 M HCl before and after addition of the green inhibitors. Figure 9(a) represent the micrograph obtained of polished MS without being exposed to the corrosive environment while Figure 9(b) showed strongly damaged MS surface due to the formation of corrosion products after immersion in 1 M HCl solution. SEM images of MS surface after immersion in 1 M HCl with 500ppm ME, HP and CP are shown in Figures9(c, d and e). It could be seen that no pits and cracks are observed in the micrographs after immersion of MS in 1 M HCl in the presence of inhibitors except polishing lines. Thus, it revealed the presence of a good protective film upon adsorption of inhibitor molecules onto the MS surface, which was responsible for the inhibition of corrosion.
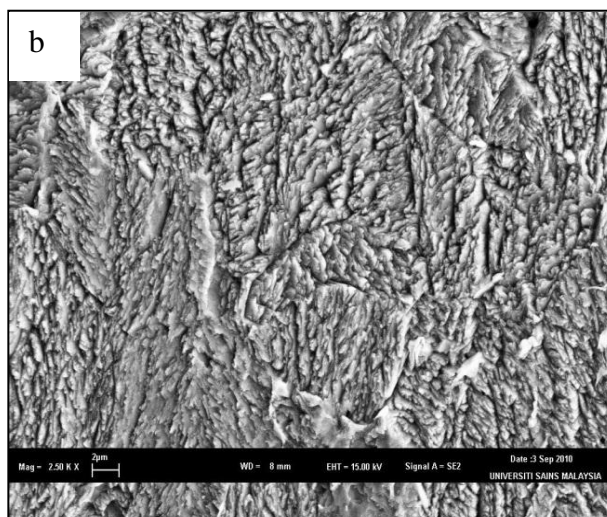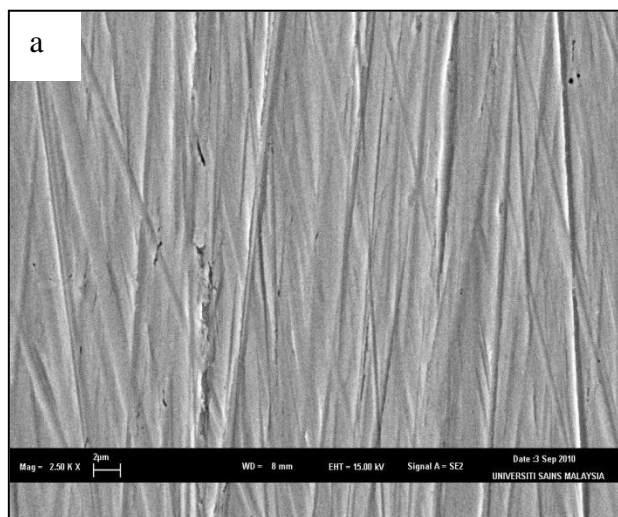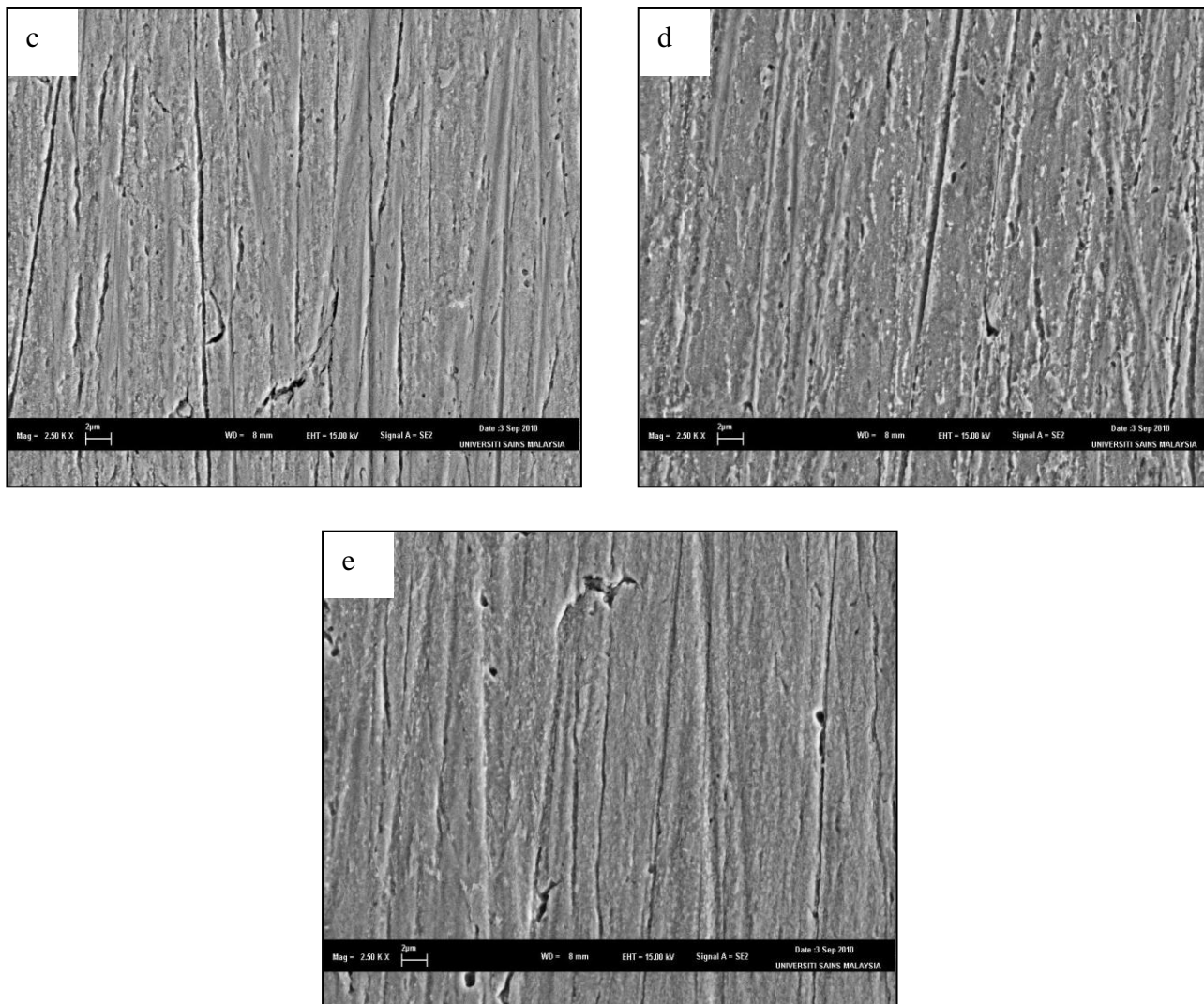
Figure 9. SEM images of MS (a) Polished MS, (b) MS in 1 M HCl, (c) MS in 1 M HCl with ME (500 ppm), (d) MS in 1 M HCl with HP (500 ppm), (e) MS in 1 M HCl with CP (500 ppm)

3.5. Adsorption isotherm

Basic information on the interaction between the inhibitors and the MS surface can be provided by the adsorption isotherm. In order to obtain the isotherm, the surface coverage values (θ) (defined as $\theta = \%\,\text{IE}/100$) were evaluated by using the %IE values obtained from weight loss, potentiodynamic and EIS studies. The θ values increased with increasing inhibitor concentration as a result of more inhibitor molecules adsorption on the metal surface. The θ values for different concentrations of ME, HP and CP were tested by fitting to several adsorption isotherms including Temkin, Langmuir, and Frumkin. For all three methods used in this study (weight loss, potentiodynamic and EIS), all inhibitors best fitted the Langmuir isotherm (Figure 10). This isotherm assumed that the adsorbed molecules occupied only on one site and there was no interaction with other molecules adsorbed. Under these circumstances, the proportionality between θ and bulk concentration (C) of the adsorbing inhibitors is as follows [37].

$$KC = \frac{\theta}{1 - \theta} \tag{5}$$

Here K is the equilibrium constant. It is convenient to rearrange the equation, yielding:

$$\frac{C}{\theta} = C + \frac{1}{K} \tag{6}$$

Figure 10 gives the result of Langmuir's plot for corrosion inhibition data of the inhibitors. Linear plots of C/θ against the C were obtained with the slope in the range of 1.00 to 1.12 which is close to unity. These results suggest that the inhibitor occupies about 1.00 to 1.12 adsorption sites on the MS surface [38]. Besides, the results show that all the linear correlation coefficients (R^2) were almost equal to unity. Thus, the adsorption phenomenon of inhibitors into the mild steel surface obeys the Langmuir isotherm.

The equilibrium constant, K is related to the free energy of adsorption (ΔG_{ads}) at a single temperature as reported [39-41]. The value of ΔG_{ads} was calculated by Eq. 7.

$$\Delta G_{ads} = -RT \ln (1000 \, K) \tag{7}$$

Where 1000 is the concentration of water in solution expressed in g/L, R is the molar gas constant and T is the temperature (27±2 °C).

The calculated values are given in Table 4. The values of ΔG_{ads} from the different techniques used for all inhibitors were in good agreement with each other. The negative values of ΔG_{ads} are an indication of the spontaneous adsorption of inhibitor on the MS surface [37].

Table 4. The values of free Gibs energy of adsorption calculated using different studies results of ME, HP and CP.

Inhibitors	Methods	Slope	R^2	K (g/L)	ΔG_{ads} (kJ mol^{-1})
ME	Weight loss	1.09	0.9975	17.21	-24.33
	Potentiodynamic	1.02	0.9948	15.43	-24.05
	EIS	1.12	0.9986	21.46	-24.88
HP	Weight loss	1.02	0.9987	18.32	-24.48
	Potentiodynamic	1.00	0.9869	11.43	-23.31
	EIS	1.08	0.9914	16.56	-24.23
CP	Weight loss	1.06	0.9994	138.9	-29.53
	Potentiodynamic	1.08	0.9999	98.04	-28.67
	EIS	1.03	0.9994	39.84	-26.42

Generally values of ΔG_{ads} around -20 kJ mol^{-1} or lower are consistent with electrostatic interactions between the charged metal and ions in solution (physisorption). Those more negative than

-40 kJ mol^{-1} involve charge sharing or charge transfer from the inhibitor molecules to the mild steel surface to form a coordinate type of bond (chemisorption) [42]. In this study, the calculated ΔG_{ads} values of ME, HP and CP that ranged from -23.31 to -29.53 kJ mol^{-1}, indicated that the adsorption mechanism was mainly physisorption. The highest ΔG_{ads} value (29.53 kJ mol^{-1}) was obtained from weight loss study of CP suggesting that this inhibitor was more strongly adsorbed onto the MS surface compared to ME and HP.
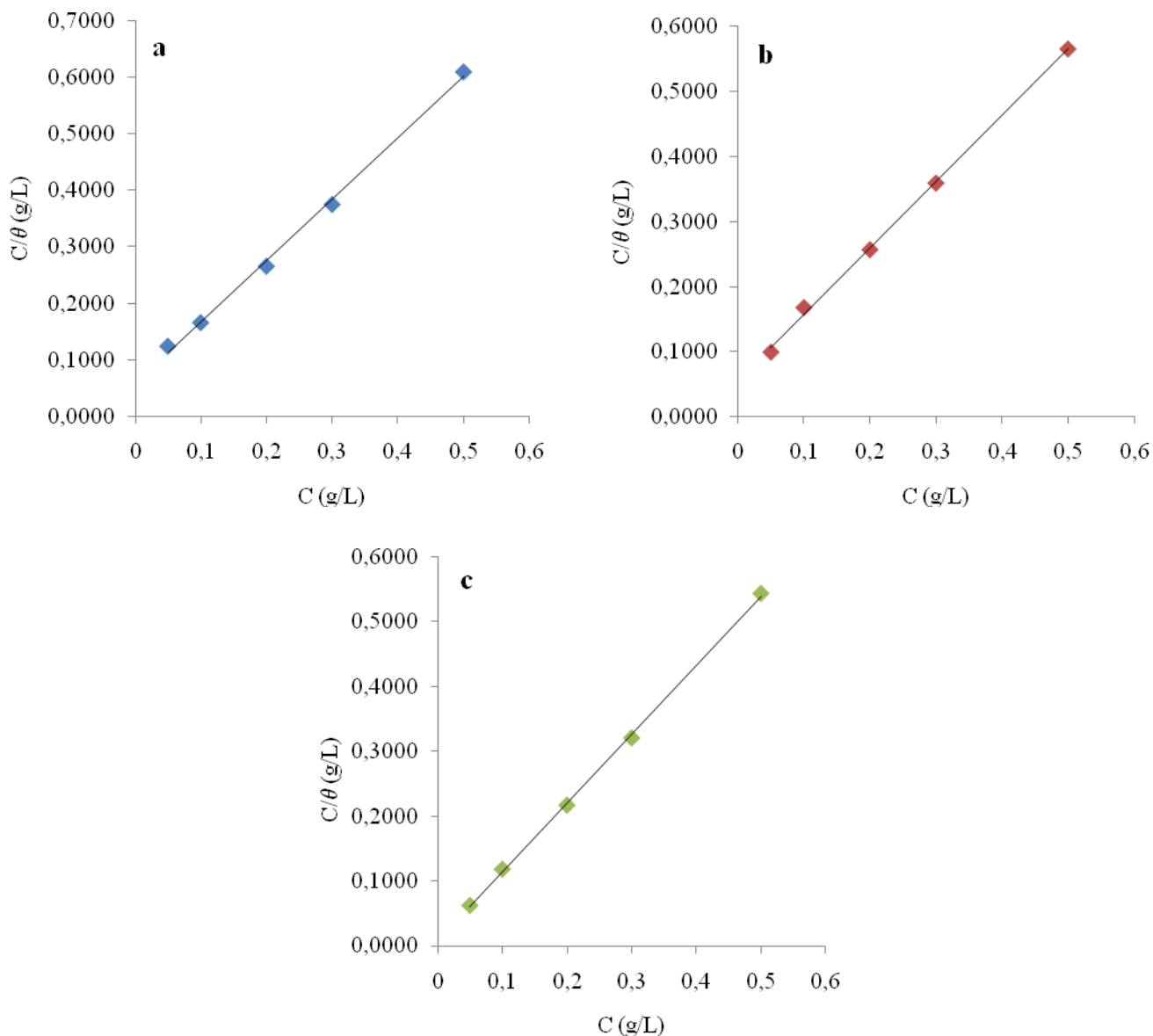

Figure 10. Langmuir isotherm for adsorption of different inhibitors on the MS surface from weight loss data: (a) ME, (b) HP and (c) CP.

3.6. Mechanism of inhibition

Previous study reported that *X. ferruginea* were tested positive for alkaloids and were found to contain atheroline alkaloids [23]. All inhibitors showed positive test with the Mayer's reagent which

confirmed the presence of alkaloids. The presence of atheroline alkaloids in the inhibitors was generally identified by using ^{1}H-NMR and FTIR. Examination of the ^{1}H-NMR spectrum of all inhibitors showed a set of aromatic proton signals in the region of δ 6.5 to 8.0 and δ 3.5 to 4.0 for O-Me groups. Besides, FTIR spectrum also proved the presence of aromatic rings in the inhibitors (Figure11). The C=C stretching bands for aromatic ring appeared between 1634 and 1464 cm^{-1}. The presence of O-Me group was also supported by the FTIR bands at about 1383 to 1075 cm^{-1}. Moreover, a broad band of the FTIR spectrum at 3400 cm^{-1} indicated the presence of N-H/O-H groups in all inhibitors. However, the adsorption of N-H of amines (δ 0.5 to 5.0) and amide (δ 5.0 to 9.0) groups by ^{1}H-NMR is not a reliable method to be used especially for crude samples. The adsorptions are highly variable depending not only on their environment in the molecule, but also on temperature and the solvent used [43].

From the %IE of weight loss, potentiodynamic and EIS studies, the results revealed that the inhibitors were excellent green inhibitors in the order of CP > NP > ME. The higher yield of creamy precipitate for Mayer's test was obtained for CP compared to NP and ME which indicated that CP contained the highest alkaloids content. Therefore, the corrosion inhibition of MS in 1 M HCl is related to the alkaloid content.

The potentiodynamic and EIS studies indicated that the inhibitors inhibit the corrosion processes by blocking the available cathodic and anodic sites of the metal surface through adsorption of the inhibitor chemical constituents on the metal surface/solution interface. This phenomenon could take place via (i) electrostatic interaction between the positively charged protonated nitrogen atoms from alkaloids and negatively charged MS surface (physisorption which occurred at cathodic sites) (ii) dipole-type interaction between unshared electron pairs of oxygen or nitrogen atoms or π electrons interaction with the vacant, low energy *d*-orbitals of Fe surface atoms (chemisorption which occurred at anodic sites) and (iii) a combination of all the above interactions (mixed type which occurred at both cathodic and anodic sites) [44].

From the adsorption isotherm study, the calculated ΔG_{ads} values of ME, HP and CP suggested that the inhibitor was adsorbed on the MS surface mainly by physisorption. However, CP was more strongly adsorbed on the metal surface. This might be due to the presence of additional N heteroatoms and phenyl groups due to the high alkaloids content. It gives additional adsorption centers, thus stronger adsorption ability on the metal surface.

The physical interaction between inhibitors and MS surface can be explained due to the presence of strongly adsorbed anions (Cl^{-}). The specific adsorption of the anions changed the MS surface into a negatively charged surface [45, 46]. Naturally, the atheroline alkaloids exist as free bases. However, due to the acidity of the corrosive medium, both N heteroatom and -NH group of atheroline alkaloids may be protonated and exist as cationic form (Figure 12) [47, 20]. Thus, the electrostatic interaction occurring between the protonated inhibitors with the negatively charged MS protected the surface from corroding. Moreover, the inhibition mechanism may also involve the chemisorption interaction. The adsorption of inhibitors may be due to a quasi-substitution process between the inhibitors in solution and water molecules at the metal surface [48].

$$Inh_{(sol)} + xH_2O_{(ads)} \leftrightharpoons Inh_{(ads)} + xH_2O_{(sol)} \tag{8}$$

Where *x* is the number of water molecule displaced by one molecule of the inhibitor. The adsorption most probably takes place through the N heteroatoms of the alkaloids. This could be due to the dipole interaction between lone pair electrons of N heteroatoms with *d*-orbitals of Fe surface atoms, forming a coordinate bond. Additionally, π electron interaction between the aromatic nucleus of the alkaloids and positively charged metal surface also plays a role [49]. However, in this study, physisorption was found to play a major role in inhibiting the corrosion of MS as shown from the adsorption isotherm studies. The results was also supported by the SEM analysis which showed smooth surface with no pits and cracks of MS treated with inhibitors in 1 M HCl as compared to without inhibitors. The inhibitors were adsorbed onto the MS surface through the alkaloids chemical constituents, forming the protective layer on the MS surface.
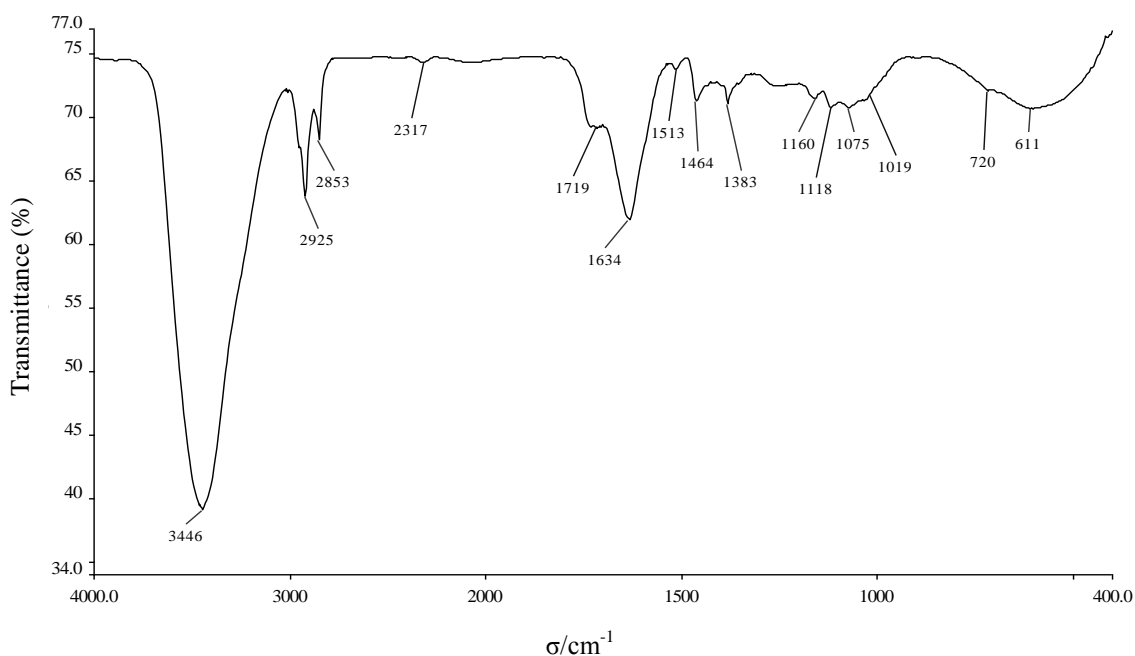
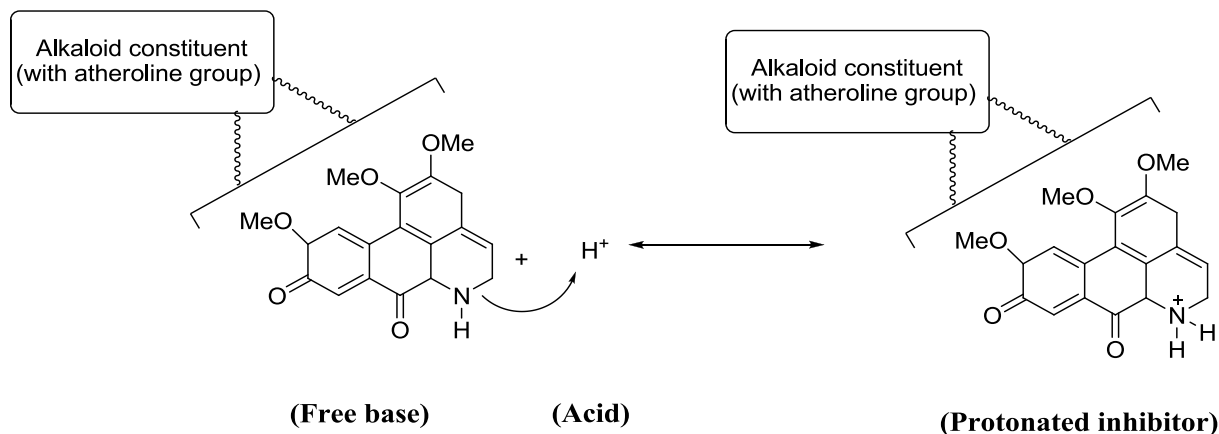**Figure 11.** FTIR absorption spectrum of CP

Figure 12. Protonated alkaloid extract in acid medium [47]

4. CONCLUSIONS

The corrosion inhibition potential of MS corrosion in 1 M HCl of *Xylopia ferruginea* was studied by weight loss, potentiodynamic polarization, EIS and SEM techniques. The main conclusions drawn from the studies are:

1)   The effectiveness of the inhibitors as corrosion inhibitors is in the order of CP > HP > ME.
2)   The inhibition efficiency increases with increasing inhibitor concentration and reaches a maximum at 500 ppm of CP.
3)   Polarization studies clearly revealed that all inhibitors acts as mixed-type inhibitors with predominant anodic effectiveness in 1 M HCl medium.
4)   AC Impedance plot of mild steel showed that as the inhibitor concentration is increased, the charge transfer resistance will increase while the capacitance double layer values will decrease.
5)   The results obtained from weight loss, polarization and impedance studies are in good agreement.
6)   SEM micrographs revealed the presence of a protective layer over the metal surface by the inhibitors through an adsorption process which obey the Langmuir adsorption isotherm. The ΔG_{ads} values of all inhibitors suggested that the inhibitors were adsorbed on the MS surface mainly by physisorption.
7)   Supporting the Mayer test, ^{1}H-NMR and FTIR studies confirmed the presence of alkaloids in the inhibitor that are related to the anticorrosion potential of the these green inhibitors.

References

1.   H.H. Uhlig and R.W. Revie, *Corrosion and corrosion control*, Wiley, New York (1985).
2.   H.A. Sorkhabi, D. Seifzadeh and M.G. Hosseini, *Corros. Sci.*, 50 (2008) 3363.
3.   F. Farelas and A. Ramirez, *Int. J. of Electrochem. Sci.*, 5 (2010) 797.
4.   X. Joseph Raj and N. Rajendran, *Int. J. Electrochem. Sci.,* 6 (2011) 348.
5.   P.K. Gogoi and B. Barhai, *Int. J. Electrochem. Sci.,* 6 (2011) 136.
6.   M.A. Quraishi and D. Jamal, *J. Appl. Electrochem.*, 32 (2002) 425.
7.   M. Elayyachy, A. El Idrissi and B. Hammouti, *Corros. Sci.,* 48 (2006) 2470.
8.   K.C. Emregül and M. Hayvalí, *Corros. Sci.*, 48 (2006) 797.
9.   B. Mernari, H. Elattari, M. Traisnel, F. Bentiss and M. Lagrenee, *Corros. Sci.*, 40 (1998) 391.
10. L. Wang, *Corros. Sci.,* 43 (2001) 2281.
11. M.E. Azhar, M. Mernari, M. Traisnel, F. Bentiss and M. Lagrenee, *Corros. Sci.,* 43 (2001) 2229.
12. W. Li, Q. He, C. Pei and B. Hou, *Electrochim. Acta*, 52 (2007) 6390.
13. W. Li, X. Zhao, F. Liu and B. Hou, *Corros. Sci.*, 50 (2008) 3261.
14. S. Ramesh, S. Rajeswari and S. Maruthamuthu, *Mater. Lett.*, 57 (2003) 4547.

15. E. Stupnisek-Lisac and S. Podbrscek, *J. Appl. Electrochem.*, 24 (1994) 779.
16. K. Srivasthava and P. Srivasthava, *Corros. Prev. Control*, 27 (1980) 5.
17. R.M. Saleh, A.A. Ismail and A.A. El-Hosary, *Corros. Prev. Control*, 31 (1984) 21.
18. B.C. Jain and J.N. Gour*, J. Electrochem. Soc.*, 27 (1978) 165.
19. M. Dahmani, A. Et-Touhami, S.S. Al-Deyab, B. Hammouti and A. Bouyanzer, *Int. J. Electrochem. Sci.,* 5 (2010) 1060.
20. M. Lebrini, F. Robert and C. Roos, *Int. J. of Electrochem. Sci.*, 5 (2010) 1698.
21. J. Sinclair, *A Revesion of Malayan Annonaceae*, Gardens Bull., Singapore (1955).
22. K. Mat-Salleh and F. Ahmad, *Proceedings of the Seminar on Malaysian Traditional Medicine*, Kuala Lumpur (1988).
23. M. Kamaliah, A.H.A. Hadi and K. Shaari, *Malaysian Journal of Science*, 12 (1990) 53.
24. S. Martinez and M. Metikos-Hucovic, *J. App. Electrochem.*, 33 (2003) 1137.
25. Y. Yan, W. Li, L. Cai and B. Hou, *Electrochim. Acta*, 53 (2008) 5953.
26. J. Cruz, T. Pandiyan and E.G. Ochoa, *J. Electroanal. Chem.*, 8 (2005) 583.
27. D.F. Roeper, D. Chidambaram, C.R. Clayton and G.P. Halada, *Electrochim. Acta*, 53 (2008) 2130.
28. Y. Tang, X. Yang, W. Yang, R. Wan, Y. Chen and X. Yin, *Corros. Sci.*, 52 (2010) 1801.
29. E. Mc-Cafferty and N. Hackerman, *J. Electrochem. Soc.*, 119 (1972) 146.
30. M.A. Quraishi and R. Sardar, *J. Appl. Electrochem.*, 33 (2003) 1163.
31. P. Bommersbach, C. Alemany-Dumont, J.P. Millet and B. Normand, *Electrochim. Acta*, 51 (2005) 1076.
32. A.V. Benedetti, P.T.A. Sumodjo and K. Nobe, *Electrochim. Acta*, 40 (1995) 2657.
33. H. Ashassi-Sorkhabi, D. Seifzadeh and M.G. Hosseini, *Corros. Sci.*, 50 (2008) 3363.
34. M.A. Quraishi, A. Singh, V.K. Singh, D.K. Yadav and A.K. Singh, *Materials Chemistry and Physics*, 122 (2010) 114.
35. Z. Tao, S. Zhang, W. Li and B. Hou, *Corros. Sci.*, 51 (2009) 2588.
36. A.Y. El-Etre, M. Abdullah and Z.E. El-Tantaury, *Corros. Sci.*, 47 (2004) 385.
37. M.G. Hosseini, S.F.L. Mertens and M.R. Arshadi, *Corros. Sci.*, 45 (2003) 1473.
38. L. Larabi, Y. Harek, O. Benali and S. Ghalem, *Progress in Organic Coatings*, 54 (2005) 256.
39. P. Lowmunkhong, D. Ungthararak and P. Sutthivaiyakit, *Corros. Sci.*, 52 (2010) 30.
40. A.M. Abdel-Gaber, B.A. Abd-El-Nabey and M. Saadawy, *Corros. Sci.*, 51 (2009) 1038.
41. S.A. Umoren, Y. Li and F.H. Wang, *Corros Sci.*, 52 (2010) 1777.
42. F. Bentiss, M. Lebrini, M. Lagrenee, M. Traisnel, A. Elfarouk and H. Vezin, *Electrochim. Acta*, 52 (2007) 6865.
43. L.P. Donald, M.L. Gary, S.K. George and R.V. James, *Introduction to spectroscopy*, Brooks/Cole, United State (2009).
44. D. Schweinsgberg, G. George and H. Nishihara, *J. Electrochem. Soc.*, 137 (1990) 1354.
45. Z.A. Iofa, V.V. Batrakov and Cho-Ngok-Ba, *Electrochim. Acta*, 9 (1964) 1645.
46. A. Frignani, F. Zucchi and C. Monticelli, *Br. Corros. J.,* 18 (1983) 19.
47. P.B. Raja and M.G. Sethuraman, *Mater. Lett.*, 62 (2008) 113.
48. J.O. Bokris and D.A.J. Swinkels, *J. Electrochem. Soc.*, 11 (1964) 736.
49. G. Trabenelli and F. Mansfeld (Eds.), *Corrosion Mechanisms*, Marcel Dekker, New York (1987).